# Integrated transcriptomic and proteomic analysis reveal new insights into stone cell formation in Korla pear

**Aisajan Mamat** ( 103326533@qq.com )
Xinjiang Academy of Agricultural Sciences https://orcid.org/0000-0002-6330-7398
**Xiaoli Zhang**
Xinjiang Academy of Agricultural Sciences
**Juan Xu**
Xinjiang Academy of Agricultural Sciences
**Peng Yan**
Xinjiang Academy of Agricultural Sciences
**Chuang Mei**
Xinjiang Academy of Agricultural Sciences
**Jixun Wang**
Xinjiang Academy of Agricultural Sciences

**Research article**

**Keywords:** Korla pear, Stone cell, Transcriptomics, Proteomics, Fruit pulp

**Posted Date:** May 12th, 2020

**DOI:** https://doi.org/10.21203/rs.3.rs-23121/v1

# Abstract

Background Korla fragrant pear(*P•sinkiangensis* Yü)is a famous local variety of Xinjiang China. One difficulty is the high stone cell content of these pears, which causes the formation of rough skins on the fruit. To elucidate the underlying mechanisms of stone cell formation, parallel analyses of the transcriptome and proteome was performed to identify important regulators and pathways involved in stone cell formation.

Results Fruit samples were collected at three important time points depending on the stages of stone cell formation (20, 50 and 80 days after flowering). A total of 24268 differentially expressed genes (DEGs) and 1011 differentially accumulated proteins (DAPs) were identified from all the time points. Function analysis of the differential genes/proteins revealed that a set of candidates was associated with stone cell formation. These candidates mainly enriched in pathways involved in lignin biosynthesis, cellulose and xylan biosynthesis, S-adenosylmethionine (SAM) metabolic process, Reactive oxygen species (ROS) production, and cell death. We mined a total of 253 DEGs, and 100 DAPs, 63 of which were significantly changed at both the transcript and protein levels during fruit development.

Conclusions Our findings reveal that some intriguing genes/proteins were previously unrecognized related with the sclereid formation, which provided new insights into molecular processes regulating sclereid accumulation in pear pulp.


# Background

Korla fragrant pear (*Pyrus sinkiangensis* yu) is a native species of the Xinjiang Autonomous Region in China. It is distinctive for its aroma, rich juicy flesh and crisp texture. At present, increasing stone cell content, which leads to the formation of rough skin fruits, is one of the most important factors that results in decreased quality. In normal fruits, stone cells are almost imperceptible, but in rough skin fruits, the lignified cell walls of the stone cells do not change during fruit maturation, and they impart a very gritty texture. Previous studies showed that stone cell are a type of sclerenchyma cells formed by secondary thickening of cell walls, and formation of stone cells is closely related to the synthesis, transfer and deposition of lignin[1–2]. Secondary walls are mainly found in tracheary elements and fibers in the xylem. Secondary wall-containing cell types are also present in sclereids in pear fruits [3–4]. The major components of secondary walls are cellulose, hemicelluloses (xylan and glucomannan) and lignin and their proportion may vary among different plant species and even in different secondary wall-containing cell types of the same species [3, 5–6]. While we understand a great deal of the genes involved in lignin synthesis and deposition [7–11], and how the corresponding genes are transcriptionally regulated, we know surprisingly little concerning the transition of the primary to secondary cell wall synthesis. Understanding how stone cells develop in pear fruit is therefore of significant biological interest.

Cellulose represented about half of stone cell walls [4]. Xylans were the main hemicellulose especially for stone cells. Stone cells contained high levels of xylose and lignin than parenchyma cells. Therefore,

formation of stone cells cannot be fully explained by the deposition of lignin in the secondary cell walls. After their biosynthesis, lignin monomers must be transported to the cell wall where they are oxidized for polymerization. Reactive oxygen species (ROS) plays a key role in this process [12–14]. In our early research, we found that, apoptosis occurs along with the development of stone cells during the fruit development, and the apoptosis period basically overlaps with the period of stone cell formation and ROS accumulation [15]. ROS is the main stress factor leading to apoptosis. Therefore, our hypothesis is that formation of stone cells is essentially the process of apoptosis triggered by ROS. $H_2O_2$ by increasing cross-linking of polymers induces stiffening of the cell wall, leading to growth inhibition in some parenchyma cells. As a result, some parenchyma cells are forced to onset of differentiation. However, little data was available on pear stone cell wall formation taking into account cell wall polymer synthesis and the cross-linkage among them. In order to reveal this scientific problem and theoretical inference, in this study, parallel analyses of the transcriptome and proteome of Korla pear fruits from the three developmental stages were carried out using RNA-seq and TMT technologies, aiming to identify differential genes/proteins that may be involved in the formation of stone cells. Our integrated omics data (transcript-protein) revealed several new and interesting insights regarding pear fruit stone cell formation. Knowledge gained through this study could be helpful for understanding the molecular mechanisms of stone cell formation in pear and could be further used to develop strategies to reduce or eliminate the probability of stone cell formation.

## Results

# Physiological and morphological changes

Stone cell staining and cell apoptosis detection results as well as cell wall polymers (cellulose, hemicellulose, lignin and polysaccharide) composition in the stone cell is shown (Fig. 1) to illustrate the difference between experimental time stages. Greater differences for stone cell, cell apoptosis and cell wall polymers composition were observed in Day20 compared to fruits sampled in later stage. It is evident from the figure that stone cell formation mainly occurred during the early stage of fruit development, and the apoptotic period basically overlapped with the period of stone cell formation (Fig A,B). On the other hand, the main components for pear stone cells were cellulose (52%) representing about half of stone cell biomass, hemicellulose (23%), lignin (20%) as well as a little amount of polysaccharide (3%). Therefore, formation of stone cells cannot be fully explained by the deposition of lignin in the secondary cell walls. In the later section, we will pay close attention on the enrichment of genes and proteins related to secondary cell wall polymer synthesis.

# Overview of transcriptomic and proteomic data

In order to identify differential genes/proteins that may be involved in stone cell formation in Korla pear, combined transcriptome and proteome analysis were performed by the RNA-seq and the TMT techniques. A total of 42893 transcripts and 7904 proteins were obtained, respectively, in which 24268 genes and

1011 proteins were showed differential expression during the developmental time course. Correlation analysis showed that approximately 13% (1010/7904) of the proteins correlated with DEGs, including 700 DAPs. Of the 1011 DAPs, 311 DAPs (30.8%) were not correlated with DEGs (Fig. 2A). The analysis of DEGs and DAPs in our study focused on pathways that involved in lignin biosynthesis (94 genes and 31 proteins), cellulose and xylan biosynthesis (46 genes and 18 proteins), SAM metabolic process(10 genes and 3 proteins), apoplastic ROS production (16 genes and 2 proteins), and cell death (14 genes and 6 proteins) (Fig. 2B). Information on all DEGs and DAPs on these pathways can be found in Data S1–S3. However, information provided in the text included genes and proteins with relatively high expression that were differentially expressed during the developmental time course (Fig. 3–5). To validate the RNA-seq results, 15 genes were randomly selected from the DEGs for qPCR analysis in the transcript levels of three time courses. As shown in Figure S1, a high agreement was observed between the RNA-seq and qPCR data, demonstrating the validity of RNA-seq data of genes with different transcript abundance.

# DEGs and DAPs involved in lignin biosynthesis

Omics data revealed that 94 DEGs and 31 correlated DAPs encoding several monolignol biosynthetic enzymes were identified in Korla pear pulp (Data S1). These genes and proteins encodes upstream enzymes of phenylpropanoid pathway (PAL, C4H, C3'H,4CL, HCT, CSE and CCoAOMT ), enzymes in the monolignol-specific pathway ( CCR, COMT, F5H and CAD) and enzymes involved in lignin polymerization (PRX, LAC). Majority of these genes showed peak expression in the early stage of fruit development, and gradually down-regulated from Day20 to Day80, showed similar trends with lignin content in pear during fruit development. Some transcripts, however, showed no differential expression from Day 50 to Day 80, indicating that lignin accumulation mainly occured in the early stage of fruit development. Interestingly, expression patterns of some transcripts encoding PAL (one transcript), C4H (two transcripts), 4CL (two transcripts), HCT (one transcript) and CCR (five transcripts), CAD (two transcripts), CSE (two transcripts) and PRX (five transcripts) showed the opposite trend, indicating that they may be involved in the biosynthesis of other secondary metabolites in the phenylalanine pathway. However, the expression levels of these genes were almost negligible, compared with expression levels of the genes positively regulated with lignin content.

### DEGs and DAPs associated with cellulose and xylan biosynthesis

Cellulose, consisting of linear chains of $\beta$-1, 4-linked glucosyl residues, is the predominant constituent of secondary cell walls. 29 DEGs in transcriptome profile were assigned to cellulose biosynthesis during the experimental time course, while 7 DAPs in proteome data (Fig. 4). UDP-glucose is the direct precursor for cellulose. Therefore pathways that lead to UDP-glucose production can potentially have an impact on cellulose biosynthesis

UDP-glucose pyrophosphorylase (UGPs) and sucrose synthase (SuSy) are the main enzymes that have been shown to produce UDP-glucose in plants [16]. But we didn't find any differential expressed genes encoding UGPs. We found 4 DEGs and 1 DEP that encodes sucrose synthase (SuSy) and their expression

pattern were the same trend as in cellulose content, indicating that SuSy tightly associated with the processes of cellulose biosynthesis. Sucrose can be directly converted to UDP-Glcose and fructose by SuSy, Hexose phosphates pool can also have an effect on UDP-glucose pool size [17]. Fructose is a feedback inhibitor of sucrose synthase, and fructokinase(FRK)phosphorylate fructose to produce fructose-6-phosphate. In our omics data, 4DEGs and 2 DEP that encode FRK were selected. All of these genes and proteins showed similar expression as *SuSy* during the experimental period, indicating that FRK might indirectly affect cellulose production through modulation of sucrose synthase activity and UDP-glucose production by reducing intracellular fructose pools. Cellulose synthase (CesA) use UDP-glucose as substrate for the biosynthesis of cellulose chains. In *arabidopsis CESA1*, *CESA3* and *CESA6* (or *CESA6-like*) are required for primary wall cellulose synthesis whereas *CesA4*, *CesA7*, *CesA8* constitute the secondary wall CesA complexes. In our study, we obtained a total of 21 functional genes and 4 proteins encoding different CesAs enzymes and cellulose synthase like proteins (CSLs), among which homologous genes of *arabidopsis CesA4* (2 transcripts), *CesA7* (2 transcripts), *CesA8* (2 transcripts) showed the same expression patterns as the genes related to lignin synthesis, in accordance with trends of lignin and stone cell contents (Fig. 1), suggesting that these genes and proteins might be involved in the development of stone cells in Korla pear pulp. However, homologous genes of *arabidopsis CesA1* (2 transcripts), *CesA2* (2 transcripts), *CesA3* (2 transcripts) and most of the *CSLs* (5 transcripts) showed the opposite trend, indicating that these genes mainly participate in the growth of primary walls of parenchyma cells in Korla pear pulp. In addition we screen for 2 DEGs and 1DEP encodes COBRA-like4 proteins (*COBL4*). *COBRA*, encodes a glycosyl-phosphatidylinositol-anchored protein, is involved in the orientation of deposition of cellulose microfibrils. In *arabidopsis COBL4* is required for cellulose synthesis in the secondary cell wall. Expression trends of these genes were similar to that of *CesA* genes associated with secondary wall synthesis, implying that this protein likely be involved in the assembly of cellulose synthase complexes.

Xylans are mainly composed of a linear backbone of β-(1, 4)-linked D-xylosyl residues. UDP-xylose is a nucleotide sugar required for xylan backbone elongation. Similarly, 25 DEGs and 13 DAPs were identified as xylan biosynthetic genes and proteins that showed the same expression trends as the genes related to cellulose and lignin synthesis (Fig. 4). These genes and proteins encoding a suite of enzymes that is required for the UDP-xylose formation, xylan backbone elongation, side chain addition and modification as well as the reducing end sequence. Among these, 1 gene with no correlated protein encodes UDP-Glucose dehydrogenase(UGD), which is an enzyme converting UDP-glucose to UDP-glucuronic acid in an irreversible manner; 6 genes and 4 proteins encodes UDP-Xylose synthase (UXS), which irreversibly convert UDP glucuronic acid to UDP-xylose; 4 genes and 4 correlated proteins encodes xylosyltransferases (XylT) required for elongation of xylan backbone; 4 genes with no correlated proteins encodes glucuronosyltransferase (*GUXs* ) required for the addition of both glucuronic acid and 4-O-methylglucuronic acid branches to xylan backbone; 6 genes and 3 correlated proteins encode glucuronoxylan 4-O-methyltransferase (GXMT ) which is responsible for the glucuronic acid (GlcA) side chain methylation in xylan; 3 genes (*IRX7*) with one correlated proteins required for formation of the xylan reducing end sequence (XRES) which has been speculated to act as either a primer or terminator for

glucuronoxylan biosynthesis[18] (Fig. 4 and Data S2). Based on the data in Fig. 4, expression levels of genes related to UDP-Xylose formation (*UXS*s), elongation of xylan backbone (*IRX*s) and side chain methylation (*GXM*s) were significantly higher than other xylan related genes, implying their important roles in xylan or glucuronoxylan synthesis. Most of secondary wall genes and xylan related genes were preferentially accumulated on Day20, while primary wall genes were relatively abundant on Day80 (Data S2). These results suggested that greater secondary thickening in parenchymal cells was occurred in the early stage of fruit development.

# Other genes and proteins involved in secondary cell wall biosynthesis

Genes involved in apoplastic ROS production (16 genes and 2 proteins), SAM metabolic process (10 genes and 3 proteins), and cell death (12 genes and 6 proteins) were well represented in the candidate gene lists (Fig. 5 and Data S3). Apoplastic ROS can be used as an oxidant in cell wall cross-linking, and are required for lignin polymerization. ROS being a major stress factor also play an important role in apoptosis induction. Apoplastic ROS related genes and proteins were preferentially accumulated in Day20, with significantly lower expression in later stages. For example, 3 genes and 1correlated protein annotated as respiratory burst oxidase homolog (RBOH) were expressed at high levels in the early stage then were down-regulated to varying extents. More accumulation of transcripts of genes encoding superoxide dismutase (SOD), polyamine oxidase (PAO), PRXs and germin-like proteins (GLPs), was also observed in the early stage of fruit development.

Genes encoding enzymes that related to S-adenosylmethionine (SAM) metabolic process were differentially expressed during fruit development in a similar manner as ROS related genes (Fig. 5 and Data S3). SAM acts as a methyl group donor for various biologically important processes including the synthesis of cell wall polymers. Moreover, SAM acts as amino carboxylpropyl group donor in polyamine generation, which is an important substrate for apoplastic $H_2O_2$ production. Numerous genes related to programmed cell death were also expressed in pear pulps, and all showed their highest expression in Day20 consistent with the trends of ROS generating genes during fruit development (Fig. 5 and Data S3).

# Discussion

Stone cells are a type of sclerenchyma cell formed by the secondary thickening of cell walls followed by the deposition of lignin on the primary walls of parenchyma cells [19–21]. Our results showed that stone cell formation mainly occurred during the early stage of fruit development. Similar results have been reported in other pear varieties [1, 2, 11]. In plant secondary walls, i.e. the proportion of cellulose, hemicelluloses and lignin, may vary among different plant species and even in different cell types of the same species. Some specialized secondary walls may be composed predominantly of one or two polymers. For example, cotton fibers contain > 90% cellulose, and phloem fibers, on the other hand, contains no lignin [6]. We found that pear stone cells mainly composed of cellulose (52%), hemicellulose (23%), lignin (20%) as well as a little amount of polysaccharide (3%). Our results are supported by several

early reports in pear [4, 22], indicating that the stone cell formation is more likely to result from the differentiation of distinct cell types.

Lignification is an integral part of the differentiation process of several specialized cell types to fulfil their physiological function [13]. Lignification process is vary among different cell type, for instance, differentiation process in tracheary elements (TEs) require cell death to achieve their lignification, in which enzymes and/or substrates required for cell wall lignification was provided by neighbouring cells [23–24]. In contrast to TEs, lignification in fibre cells is carried out by cell autonomous processes [23–24]. Lignin composition varies among these cell types, in TEs, mainly composed of G-units, and the sclerenchyma fibres have lignified secondary cell walls mainly composed of S-units [25–26]. In our previous research, we found that sinapyl alcohol, which gives rise to S-unit, was the dominant lignin monomer in Korla pear pulp, accounting for 77.2% of total alcohol monomer [21]. These observations have led to the idea that stone cell differentiation in pear pulp might proceed through in a cell-autonomous process. Since lignification in sclerenchyma fibre cells begins with a microtubule-dependent deposition of xylan and cellulose in the secondary cell wall. Therefore being a type of sclerenchyma, differentiation of stone cells must begin with a cellulose and xylan secondary cell wall deposition. Supporting this theory, we found that many secondary cell wall genes and proteins (53 genes and 20 proteins) showed peak expression in the early stage of fruit development, consistent with the changing trends of stone cell and lignin.

Cellulose is the load-bearing unit, in which cellulose microfibrils cross-link with hemicelluloses to form the framework of secondary walls. We found that cellulose content accounted for more than a half of stone cell biomass, indicating that it plays a decisive role in the differentiation of stone cells. Cellulose synthase (CesA) use UDP-glucose as substrate for the biosynthesis of cellulose chain [27–28]. Therefore, pathways that lead to UDP-glucose production can potentially have an impact on cellulose biosynthesis. SUSs and UGPs are the main enzymes that produce UDP-glucose in plants [16]. In our study, we found 4 DEGs and 1 DEP that encodes SuSy. It is reported that in hybrid aspen inhibition of the SuSy activity reduced carbon allocation to all the secondary cell wall polymers, however, its over expression only increased cellulose deposition in hybrid poplar [29–30]. In accordance with these findings, in our present work several genes encoding SuSy in pear pulp showed peak expression in Day20, then down-regulated more than 20-fold in Day80 in parallel with cellulose content, indicating that SuSy tightly associated with the processes of cellulose biosynthesis. In our early research, we found that SuSy expressed higher enzymatic activity in the early stage of fruit development in Korla pear, SuSy activity decreased first and then increased gradually 60 days after flowering. Accordingly, sucrose accumulations rose slowly in the later stage,began to increase 60 days after flowering [31], suggesting that in the early stage of fruit development sucrose are mainly used to cellulose synthesis. Fructose is a feedback inhibitor of SuSy [17]. FRK phosphorylate fructose to produce fructose-6-phosphate.We identified 4DEGs and 2 DEP that encode FRK showed similar expression as *SuSy* during the experimental period, indicating that FRK might indirectly affect cellulose production through modulation of SuSy and UDP-glulcose production by reducing intracellular fructose pools [16–17, 32].

In our study, *CESA* genes that encode cellulose synthases were differentially expressed during the experimental time course. As expected, genes encoding CESAs that are involved in secondary cell wall cellulose synthesis [33–34] (*CESA4*, *CESA7* and *CESA8*) showed peak expression in the early stage of fruit development and gradually decline in expression in the later stage. In contrast, genes required for primary wall cellulose synthesis [33–34] (*CESA1*, *CESA2* and *CESA3*) expressed the opposite trend. In addition correlated proteins of *AtCESA7* and *AtCESA8* were also found to be differentially expressed during the experimental time course, and showed the same trend as their corresponding genes. It has been demonstrated that presence of *AtCESA4*, *AtCESA7* and *AtCESA8*s is required for their assembly into complexes and their correct targeting to the plasma membrane [35–46]. Mutation of any of these three genes causes a severe reduction in cellulose content and secondary wall thickening [33–34]. The same results were reported in rice, brachypodium and populus [37–39]. These findings suggest that *CESA* genes required for secondary cell wall cellulose synthesis participate in the process of stone cell differentiation.

Hemicellulose is another major component of pear stone cells, accounting for 23% of stone cell biomass. Xylan, a major hemicellulosic component, is essential for secondary wall strength [40]. UDP-xylose is a nucleotide sugar required for xylan backbone elongation. UDP-xylose was formed by serial actions of UGD and UXS. Genes encoding these two enzymes showed higher expression in the early stage of development. Expression levels of UXSs were more than 100-fold higher than UGDs, indicating that UXS is the major enzyme responsible for UDP-xylose. This is supported by the evidence that antisense downregulation of UXS leads to high glucose-to-xylose ratios in xylem walls due to fewer xylose-containing polymers. Such plants also have altered vascular organization and reduced xylans in their secondary walls [41–42].

A number of enzymes have been identified as potentially involved in the elongation of the xylan backbone and its side chains addition. Coincident with expression of *CESA* genes involved in secondary cell wall biosynthesis, genes or proteins encoding secondary cell wall xylan synthesis enzymes [43–47] (*IRX10*, *IRX15*, *IRX15-L*) showed peak expression in the early stage of fruit development and down-regulated in the later stage. In Arabidopsis, all of *irx* mutants exhibit similar phenotypes, including severe reductions in xylan content and chain length and secondary wall thickness [43–47]. Interestingly, there was no significant reduction of xylan:XylT activity in *irx15* and *irx15-L* mutants, and the *irx15 irx15-L* double mutant has replacement of GlcA with meGlcA xylan side chain. Therefore, *IRX15* and *IRX15-L* define a new class of genes involved in xylan biosynthesis, whose function remains elusive [48–50].

Another group of genes involved in addition of GlcA side chains and side chain methylation such as *GUXs* and *GXMTs* showed peak expression in the early stage of fruit development, and expressed at low levels in the later stages. Our results were supported by the evidences that these genes are preferentially expressed in secondary wall-forming cells, and mutations in these genes lead to a complete loss of GlcA or methylated GlcA side chains in xylan [51–53]. Furthermore, *gux1 gux2 gux3* triple mutants also has found with an irregular xylem phenotype with reduced secondary wall thickness [52], indicating that GlcA substitution of xylan is important in maintaining wall integrity. Genes such as *FRA8*/ *IRX7*, *F8H*, *IRX8* and

*PARVUS* have been identified to be required for the biosynthesis of XRES, all of which are expressed in secondary wall-forming cells [54–56]. Consistent with this notion, we screened three DEGs and one DAP that annotated as probable *IRX7*, which were substantially up-regulated in the early stage, and down-regulated in the later stage, indicating that these genes are required for xylan synthesis. What is noticeable is that mutation in XRES related genes can't affect either XylT or GlcAT enzyme activity, despite the loss of XRES [48, 50].

Lignin comprises approximately 20% of stone cell biomass (Fig. 1). Previous studies have shown that lignin related genes are closely associated with the development of lignified xylem and interfascicular fibers in stems [57–59]. Similarly, in present study more than 90 genes and 31 proteins involved in lignin biosynthesis were differentially expressed during pear fruit development (Data S1). Majority of these genes showed peak expression in the early stage of fruit development, positively correlated with lignin content, but some transcripts showed the opposite trend. However, the expression levels of genes positively regulated with lignin content were universally much higher than that of negatively regulated genes, indicating that they are the core genes responsible for lignin synthesis during stone cell formation in pear fruits. Genes and enzymes involved in monolignol biosynthesis have been studied extensively in different pear varieties [1, 2, 8, 21, 60–61]. Therefore roles of these genes during lignin accumulation in pear pulp will not be discussed in detail. Instead, we focus mainly on the genes involved in lignin polymerization.

After their synthesis monolignols are transported into cell walls, where they are oxidized by laccases and peroxidases to form monolignol radicals, which are then polymerized into lignin by radical coupling [62–65]. In our study all of *LAC* genes and majority of *PRX* genes showed similar expression profile as monolignol biosynthetic genes. Although some *PRX* genes showed the opposite trend, their expression levels almost negligible during the entire period, compare to up regulated *PRX*s in the early stage. *LAC*s are reported to be co-regulated with monolignol synthetic genes and secondary cell wall-forming genes [50, 66]. We found that 6 of 17 *LAC* genes, three transcripts of *LAC4-L*, two transcripts of *LAC17-L* and one transcripts of *LAC2-L*, expressed 10-150-fold higher than other transcripts, indicating that these are the core *LAC*s for the formation of monolignol radicals. Mutant studies have shown that simultaneous mutation of *LAC4* and *LAC17* results in a reduction in lignin content and *lac4lac11lac17* triple mutant results in a phenotype of severe growth defect and a loss of lignification in root vessels [63, 67–68]. Like laccases, are expressed in lignifying vascular tissue.In model plant down-regulation or silencing of genes (*PRX2*, *PRX3*, *PRX25*, *PRX60*, *PRX71*, *PRX72*, *etc*) encoding peroxidases resulted in reduced lignin accumulation and altered lignin composition [65, 69]. Consistent with these findings, our study showed that six transcripts of *PRX*s (two *PRX12-L*, two *PRX42-L*, one *PRX25* and one *PRX72-L*) were expressed remarkably higher (up to several hundred times) than other transcripts throughout the experiment. Correlated proteins of *PRX12-L* and *PRX72-L* also up regulated 10-100-fold higher than other correlated proteins, suggesting their importance for lignin polymerization in Korla pear.

Beside the lignin monomers, peroxidases and laccases require $H_2O_2$ and $O_2$, respectively to form monolignol radicals. Our study showed that ROS related genes and their encoding proteins were more abundantly expressed in the early stage, and down-regulated in the later stage. Certain ROS, like H2O2, can be used as an oxidant in cell wall cross-linking, or as a signalling molecule controlling various biological processes [70–71]. It is reported that casparian strip and the sclerenchyma cells are found with an increase of $H_2O_2$. Scavenging of $H_2O_2$ reduces the lignification of the casparian strip, TEs and the extracellular lignin accumulation in cell cultures [24, 72–73]. Together these findings indicate that apoplastic ROS play important role in the lignification process (stone cell formation). $H_2O_2$ is also a key modulator of programmed cell death (PCD) which is related with a number of developmental processes including tissue (tracheary elements, fibers, ect) differentiation [74]. The present study found several highly transcribed cell death related genes and proteins (*AED3-like*, *MC1-like*, *ACD11-like*), expression pattern of which were similar to that of ROS related genes.

# Conclusions

On the basis of these multi-level results, we conclude that stone cells are mainly composed of cellulose, hemicellulose and lignin as well as a little amount of polysaccharide. In addition to lignin synthetic genes, many genes related to secondary wall development, cell apoptosis and ROS production were highly expressed during the critical period of cell differentiation. Therefore, formation of stone cells cannot be fully explained by the deposition of lignin in the secondary cell walls. Together with lignin related genes, other genes/proteins encoding enzymes responsible for the synthesis of other secondary cell wall components (cellulose, xylan) co-regulate the differentiation process of stone cells. These previously unrecognized genes/proteins provided new insights into molecular processes regulating stone cell accumulation in pear pulp.

# Methods

### Plant materials and sampling periods

Fruits of ‘Korla pear’ were obtained from 20-year-old pear trees grown on a farm (Korla, Xinjiang, China). The first author is responsible for the entire field sampling process. In the last 5 years, all of our field experiments on Korla pear have been carried out in this experimental park to ensure the consistency of plant materials and the reliability of pear variety. There is no voucher specimen of this material has been deposited in a publicly available herbarium. Three important time points were sampled depending on the stages of stone cell formation in 2018, Day20 (20 days after flowering) represents the early development stage of stone cells; Day50 (50 days after flowering) represents the later stage of stone cell formation, and Day80 (80 days after flowering) represents the stationary phase of stone cells (with lower stone cell contents ). In the early stage (Day20 and Day50), each biological replicate consisted of fifteen single fruit samples collected from five independent trees, and ten fruits were collected for each biological replicate in the later stage. The fruit skins were peeled with a peeler, and cylindrical samples, 15 mm in diameter,

were sampled from the pulp, frozen in liquid nitrogen, ground into mixed samples and stored at −80°C until further analysis. The same batch of sampling materials was used for transcriptome, proteome, physiological and biological analyses.

### Stone cell separation and structural carbohydrate detection

Stone cell separation was carried out as described by Brahem et al (2017) [4]. Briefly 2 kg of frozen pear flesh was used. The separation of stone cells from parenchymatous tissues was based on their higher density. After washing with acetone: water, the pulp was stored overnight at 4°Cin the same acetone:water (60:40, v:v) solution. Stone cells sedimented and formed a distinctive yellow layer at the bottom of the container. The stone cells were collected, oven-dried, ground into a uniform powder. The lignin content was measured using the Klason method [75]. A small amount (0.2 g) of this powder was extracted with 15 ml of 72% $H_2SO_4$ at 30°C for 1 h, combined with 115 ml of distilled water and boiled for 1 h. The volume was kept constant during boiling. The liquid mixture was filtered and the residue was rinsed with 500 ml of hot water, air-dried and weighed. The hemicellulose content was determined by 2% hydrochloric acid hydrolysis method combined with DNS method [76]. The cellulose content was determined by Anthrone-Sulfuric acid colorimetry method [76]. The polysaccharide content was tested by phenol-sulfuric acid method [77].

### Stone cell staining and apoptosis detection

Stone cells were sectioned using a procedure reported by Cai et al. (2010) [2]. Pulp, from 2.0mm under the peel was collected, cut into appropriate sizes, and fixed with FAA fixative solution (50 ml 50% ethanol, 5ml glacial acetic acid, 5ml formalin). Pulp sections were cut manually, stained with 0.1% Safranin, and studied under an optical microscope. Apoptosis was detected by TUNEL assay kits from Shanghai beyotime (www.beyotime.com). The kits were carried out according to the manufacturer's instructions.

### Transcriptomic sequencing

Transcriptomic sequencing was performed by Novogene Bioinformatics Technology Co., Ltd (Beijing, China). In brief, total RNA was isolated by use of TRIzol reagent and the purity, concentration and integrity of RNA were determined. Once RNA samples were qualified, Oligo-dT beads were used for the isolation of mRNA. After that, the isolated mRNA was fragmented into short sections and used for the synthesis of first-strand cDNA. The synthesis of second-strand cDNA was conducted by use of dNTPs, DNA polymerase I and RNase H. The purification of double-stranded cDNA was performed using AMPure XP beads, and then the purified double-stranded cDNA were used for end reparation, "A" base addition and ligation of sequencing adapters. After size selection with AMPure XP beads, PCR amplification was performed and the production was purified using AMPure XP beads for library construction. Finally, the library was sequenced as 2 × 150 bp paired-end reads on Illumina HiSeq$^{TM}$ P150 sequencer (Illumina, San Diego, CA, USA). Raw data were cleaned by removing reads with adaptors, low quality (> 50 %) or high-proportion unknown bases (> 10 %) and then were assembled by use of Trinity methodology. The

annotation of transcriptome sequences were performed using the following seven databases: Nr (NCBI non-redundant protein sequences), Nt (NCBI nucleotide sequences), Pfam (Protein family), KOG/COG (eukaryotic Ortholog Groups and Clusters of Orthologous Groups of proteins), Swiss-Prot (A manually annotated and reviewed protein sequence database), KEGG (Kyoto Encyclopedia of Genes and Genomes) and GO (Gene Ontology). The read numbers were transformed to FPKM (fragments per kilobase of transcript sequence per millions base pairs sequenced) value for gene expression quantification, and differentially expressed genes (DEGs) between day 50 and day20, day80 and day 20, and day 80 and day50 were selected based on padj< 0.05. KEGG pathway analysis was conducted and corrected Pvalue (FDR) cut-off was set at 0.05. The sequencing data have been deposited in the NCBI Sequence Read Archive (SRA) database under the accession number PRJNA588520.

## Proteomic sequencing

Proteomic sequencing was performed by Novogene Bioinformatics Technology Co., Ltd (Beijing, China). Briefly, the concentrations of proteins were determined using Bradford assay and 100 μg of protein from each replicate was digested with Trypsin Gold (Promega, Madison, WI) at 37°C for 16 h. After that, peptides were dried by vacuum centrifugation, and Desalted peptides were labeled with TMT6/10-plex reagents (TMT6/10plex™ Isobaric Label Reagent Set, Thermofisher), following the manufacturer's instructions. After labeling, the samples were mixed and lyophilized. TMT-labeled peptide mix was fractionated using a C18 column (Waters BEH C18 4.6×250 mm, 5 5μm,) on a Rigol L3000 HPLC. Eluent was collected every minute and merged to generate 15 fractions. Shotgun proteomics analyses were performed using an EASY-nLC$^{TM}$ 1200 UHPLC system (Thermo Fisher) coupled to an Orbitrap Q Exactive HF-X mass spectrometer (Thermo Fisher) operating in the data-dependent acquisition (DDA) mode. Peptides were separated on a Reprosil-Pur 120 C18-AQ analytical column (15 cm×150 μm, 1.9 μm). Full MS scans from 350 to 1500 m/z were acquired at a resolution of 60000 (at 200 m/z) with an AGC target value of $3\times10^6$and a maximum ion injection time of 20 ms. From the full MS scan, a maximum number of 40 of the most abundant precursor ions were selected for higher energy collisional dissociation (HCD) fragment analysis at a resolution of 15000 for TMT6-plex (at 200 m/z) or 45000 for TMT10-plex (at 200 m/z) with an automatic gain control (AGC) target value of $1\times10^5$, a maximum ion injection time of 45ms, a normalized collision energy of 32%, an intensity threshold of $8.3\times10^3$, and the dynamic exclusion parameter set at 60 s. Differentially accumulated proteins (DAPs) were selected based on p< 0.05 and |log2FC| > 0.585. To identify the most important biochemical metabolic pathways and signal transduction pathways involved in differentially expressed proteins, KEGG analysis were performed. GO enrichment analysis of differentially expressed proteins was performed to identify the major biological functions.

## Quantitative real-time PCR validation

Several genes which were significantly enriched in lignin, cellulose and xylan biosynthetic pathways were randomly selected for quantitative real-time PCR validation. Total RNA was isolated with TRIzol reagent (Takara, Dalian, Liaoning, China). First-strand cDNA synthesis was conducted by use of Prime Script TM

RT reagent kits (Takara, Dalian, Liaoning, China). Quantitative real-time PCR was performed using SYBR Green kits (Takara, Dalian, Liaoning, China). Primer sequences were designed with the online designing tool in NCBI (http://www.ncbi.nlm.nih.gov/tools/primer-blast/). The reaction conditions of PCR were 95 °C for 10 min, followed by 40 cycles of 95 °C for 15 s and 60 °C for 1 min. Expressions of genes were concluded by using the $2-\Delta\Delta CT$ method.

### Statistical analysis

Statistical significance of differences in this study was analyzed using one-way ANOVA followed by Tukey's post hoc test with a significance level of 0.05 ($p < 0.05$) (GraphPad Prism 7.0 software for Windows).

## Abbreviations

| | |
|---|---|
| 4CL: 4-coumarate–CoA ligase; | IRX: Irregular xylan; |
| ACD: Accelerated cell death; | LAC: Laccase; |
| AED: Aspartyl protease; | MC: Metacaspase; |
| C3'H*: ρ*-coumaroyl shikimate 3'-hydroxylase; | PAL: Phenylalanine ammonia-lyase; |
| C4H: Cinnamate 4-hydroxylase; | PAO: Polyamine oxidase; |
| CAD: Cinnamyl alcohol dehydrogenase; | PRX: Peroxidase; |
| CCoAOMT: Caffeoyl-CoA O-methyltransferase; | RBOH: Respiratory burst oxidase homolog ; |
| CCR: Cinnamoyl-CoA reductase; | RNA-seq: RNA-sequencing; |
| CesA: Cellulose synthase; | ROS: Reactive oxygen species); |
| COBL4: COBRA-like 4 proteins; | SAM: S-adenosylmethionine; |
| COMT: Caffeic acid 3-O-methyltransferase; | SAMDC: S-adenosylmethionine decarboxylase; |
| CSE: Caffeoylshikimate esterase; | SAMS: S-adenosylmethionine synthase; |
| CSLs cellulose synthase like proteins; | SAMT: S-adenosylmethionine-dependent methyltransferase; |
| DAPs: differentially accumulated proteins; | SOD: Superoxide dismutase; |
| DEGs: differentially expressed genes; | SuSy: Sucrose synthase; |
| F5H: Ferulate 5-hydroxylase; | TMT: Tandem Mass Tags; |
| FRK: Fructokinase; | UGD: UDP-Glucose dehydrogenase; |
| GlcA: Glucuronic acid; | UGPase: UDP-glucose pyrophosphorylase; |
| GLPs: Germin-like proteins; | UXS: UDP-Xylose synthase; |
| GUXs: glucuronosyltransferase; | XRES: Xylan reducing end sequence; |
| GXMT: Glucuronoxylan 4-O-methyltransferase; | XylT: Xylosyltransferases; |
| $H_2O_2$: Hydrogen peroxide | |
| HCT: Hydroxycinnamoyl-CoA-transferase; | |

# References


1. Tao ST, Khanizadeh S, Zhang H, Zhang SL. Anatomy, ultrastructure and lignin distribution of stone cells in two Pyrus species. Plant Sci. 2009;176:413–411.

2. Cai YP, Li GQ, Nie JQ, LinY, Nie F, Zhang JY, Xu YL. Study of the structure and biosynthetic pathway of lignin in stone cells of pear. Sci Hortic. 2010;125:374–9.
3. Mauseth JD. Plant Anatomy. The Benjamin/Cummings Publishing Company, Inc., Menlo Park, CA;1988.
4. Brahem M, Renard C, Gouble B, Bureau S, Bourvellec CL. Characterization of tissue specific differences in cell wall polysaccharides of ripe and overripe pear fruit. Carbohydrate Polymers. 2017;156:152–64.
5. Timell TE. Recent progress in the chemistry of wood hemicelluloses. Wood Sci Technol. 1967;1:45–70.
6. Haigler CH, Betancur L, Stiff MR, Tuttle JR. Cotton fiber: a powerful single-cell model for cell wall and cellul, ose research. Front Plant Sci. 2012;3:104. doi:10.3389/fpls.2012.00104.
7. Jin Q, Yan CC, Qiu JX, Zhang N, Lin Y, Cai YP. Structural characterization and deposition of stone cell lignin in Dangshan Su pear. Sci Hortic. 2013;155:123–30.
8. Yan C, Yin M, Zhang N, Jin Q, Fang Z, Lin Y. Stone cell distribution and lignin structure in various pear varieties. Sci Hort. 2014;174:142–50.
9. Lu GL, Li ZJ, Zhang XF, Wang R, Yang SL. Expression analysis of lignin-associated genes in hard end pear (*Pyrus pyrifolia*, Whangkeumbae) and its response to calcium chloride treatment conditions. J Plant Growth Regul. 2015;34:251–62.
10. Cao Y, Han Y, Li D, Lin Y, Cai Y. Systematic analysis of the 4-coumarate:coenzyme A ligase (4CL) related genes and expression profiling during fruit development in the Chinese Pear. Genes. 2016;7(10):89.
11. Wang Y, Zhang X, Yang S, Wang C, Lu G, Wang R, Yang Y, Li D. Heterogenous expression of Pyrus pyrifolia PpCAD2 and PpEXP2 in tobacco impacts lignin accumulation in transgenic. plants Gene. 2017;637:181–9.
12. Suzuki N, Miller G, Morales J, Shulaev V, Torres MA, Mittler R. Respiratory burst oxidases: the engines of ROS signaling. Curr Opin Plant Biol. 2011;14:691–9.
13. Barros J, Serk H, Granlund I, Pesquet E. The cell biology of lignification in higher plants. Ann Bot. 2015;115(7):1053–74.
14. Voxeur A, Wang Y, Sibout R. Lignification: different mechanisms for a versatile polymer. CurrOpin Plant Biol. 2015;23:83–90.
15. Mamat A, Zhang XL, MA K, Mei C, Yan P, Han LQ, Wang JX. Study on the relationship between the stone cell formation and apoptosis during the fruit development of Korla Xiangli Pear. J Fruit Sci. 2020;37(1):68–76. (In Chinese).
16. Mahboubi A. New insights into carbon transport and incorporation to wood. Umeå: Doctoral Thesis Swedish University of Agricultural Sciences. 2014.
17. Roach M, Gerber L, Sandquist D, Gorzsás A, Hedenströ M, Kumar M, Niittylä T. Fructokinase is required for carbon partitioning to cellulose in aspen wood. Plant J. 2012;70(6):967–77.

18. York WS, O'Neill MA. Biochemical control of xylan biosynthesis - which end is up? Curr Opin Plant Biol. 2008;11:258–65.
19. Qiao YJ, Zhang SL, Tao ST, Zhang ZM, Liu ZL. Advances in research on developing mechanism of stone cells in pear. fruit J Fruit Sci. 2005;22:367–71. (In Chinese).
20. Nie JQ, Cai YP, Zhang SH, Lin Y, Xu YL, Zhang JY. The anatomic study on relationship of stone cells and parenchyma cells during fruit development of pyrus bretschneideri. Acta Hortic Sin. 2009;36:1209–14. (In Chinese).
21. Mamat A, Ayup M, Zhang XL, Ma K, Mei M, Yan P, Han LQ, Wang JX. Pulp lignification in Korla fragrant pear. Eur J Hortic Sci. 2019;84(5):263–73.
22. Ben-Arie R, Kislev N, Frenkel C. Ultrastructural changes in the cell walls of ripening apple and pear fruit. Plant Physiol. 1979;64:197–202.
23. Smith RA, Schuetz M, Roach M, Mansfield SD, Ellis B, Samuels L. Neighboring parenchyma cells contribute to Arabidopsis xylem lignification, while lignification of interfascicular fibers is cell autonomous. Plant Cell. 2013;25:3988–99.
24. Pesquet E, Zhang B, Gorzsa´s A, et al. Non-cell-autonomous postmortem lignification of tracheary elements in Zinnia elegans. Plant Cell. 2013;25:1314–28.
25. Terashima N, Fukushima K. Biogenesis and structure of macromolecular lignin in the cell wall of tree xylem as studied by microautoradiography. Plant Cell Wall Pol. 1989; 160–168.
26. Higuchi T. Lignin biochemistry: biosynthesis and biodegradation. Wood Sci Tech. 1990;24:23–63.
27. Arioli T, Peng L, Betzner AS, Burn J, Wittke W, et al. Molecular analysis of cellulose biosynthesis in Arabidopsis. Science. 1998;279:717–20.
28. Taylor N. Cellulose biosynthesis and deposition in higher plants. New Phytol. 2008;178:239–52.
29. Coleman HD, Yan J, Mansfield SD Sucrose synthase affects carbon partitioning to increase cellulose production and altered ce all ultrastructure. Proc. Natl. Acad. Sci. USA. 2009; 106(31):13118–13123.
30. Gerber L, Zhang B, Roach M, Rende U, Gorzsás A, Kumar M, Sundberg B. Deficient sucrose synthase activity in developing wood does not specifically affect cellulose biosynthesis, but causes an overall decrease in cell wall polymers. New Phytol. 2014;203(4):1220–30.
31. Maimaiti A, Zhang XL, Mei C, Yan MAK P and Wang JX. Soluble sugar accumulation and related enzyme activity in the fruits of Korla Fragrant Pear. Xinjiang Agricultural Sciences. 2018;55(4):664–73. (In Chinese).
32. Verbančič J, Lunn JE, Stitt M, Persson S. Carbon supply and the regulation of cell wall synthesis. Mol Plant. 2018;11:75–94.
33. Taylor NG, Howells RM, Huttly AK, Vickers K, Turner SR. Interactions among three distinct CesA proteins essential for cellulose synthesis. Proc Natl Acad Sci USA. 2003;100:1450–5.
34. Timmers J, Vernhettes S, Desprez T, Vincken JP, Visser RG, F., Trindade LM. Interactions between membrane-bound cellulose synthases involved in the synthesis of the secondary cell wall. FEBS Lett. 2009;583:978–82.

35. Taylor NG, Laurie S, Turner SR. Multiple cellulose synthase catalytic subunits are required for cellulose synthesis in Arabidopsis. Plant Cell. 2000;12:2529–39.
36. Gardiner JC, Taylor NG, Turner SR. Control of cellulose synthase complex localization in developing xylem. Plant Cell. 2003;15:1740–8.
37. Tanaka K, Murata K, Yamazaki M, Onosato K, Miyao A, Hirochika H. Three distinct rice cellulose synthase catalytic subunit genes required for cellulose synthesis in the secondary wall. Plant Physiol. 2003;133:73–83.
38. Joshi CP, Thammannagowda S, Fujino T, Gou JQ, Avci U, Haigler CH, et al. Perturbation of wood cellulose synthesis causes pleiotropic effects in transgenic aspen Mol Plant. 2011;4:331–45.
39. Handakumbura PP, Matos DA, Osmont KS, Harrington MJ, Heo K, Kafle K, et al. Perturbation of Brachypodium distachyon CELLULOSE SYNTHASE A4 or 7 results in abnormal cell walls. BMC Plant Biol. 2013;13:131.
40. Simmons TJ, Mortimer JC, Bernardinelli OD, Pöppler AC, Brown SP, deAzevedo ER, Dupree R, Dupree P. Folding of xylan onto cellulose fibrils in plant cell walls revealed by solid-state NMR. Nat Commun. 2016;7:13902. doi:10.1038/ncomms13902.
41. Pan YX, Wang XF, Liu HW, Zhang GY, Ma ZY. Molecular cloning of three UDP-glucuronate decarboxylase genes that are preferentially expressed in gossypium fibers from elongation to secondary cell wall synthesis. J Plant Biol. 2010;53:367–73.
42. Du Q, Pan W, Tian J, Li B, Zhang D. The UDP-glucuronate decarboxylase gene family in Populus:structure, expression, and association genetics. PLoS ONE 2013; 8(4): e60880. doi:10.1371/journal.one.0060880.
43. Brown DM, Goubet F, Wong VW, Goodacre R, Stephens E, Dupree P, et al. Comparison of five xylan synthesis mutants reveals new insight into the mechanisms of xylan synthesis. Plant J. 2007;52:1154–68.
44. Brown DM, Zhang Z, Stephens E, Dupree P, Turner SR. Characterization of IRX10 and IRX10-like reveals an essential role in glucuronoxylan biosynthesis in Arabidopsis. Plant J. 2009;57:732–46.
45. Lee C, O'Neill MA, Tsumuray Y, Darvill AG, Ye ZH. The irregular xylem9 mutant is deficient in xylan xylosyltransferase activity. Plant Cell Physiol. 2007a; 48: 1624–1634.
46. Peña MJ, Zhong R, Zhou GK, Richardson EA, O'Neill MA, Darvill AG, York WS. and Ye Z.H. Arabidopsis irregular xylem8 and irregular xylem9: implications for the complexity of glucuronoxylan biosynthesis. Plant Cell. 2007;19:549–63.
47. Wu AM, Rihouey C, Seveno M, Hörnblad E, Singh SK, Matsunaga T, et al. The Arabidopsis IRX10 and IRX10-LIKE glycosyltransferases are critical for glucuronoxylan biosynthesis during secondary cell wall formation. Plant J. 2009;57:718–31.
48. Brown DM, Wightman R, Zhang Z, Gomez LD, Atanassov I, Bukowski JP, et al. Arabidopsis genes IRREGULAR XYLEM (IRX15) and IRX15L encode DUF579-containing proteins that are essential for normal xylan deposition in the secondary cell wall. Plant J. 2011;66:401–13.

49. Jensen JK, Kim H, Cocuron JC, Orler R, Ralph J, Wilkerson CG. The DUF579 domain containing proteins IRX15 and IRX15-L affect xylan synthesis in Arabidopsis. Plant J. 2011;66:387–400.
50. Brown DM, Leo AHZ, Ellis J, Goodacre R, Turner SR. Identification of novel genes in Arabidopsis involved in secondary cell wall formation using expression profiling and reverse genetics. Plant Cell. 2005;17:2281–95.
51. Mortimer JC, Miles GP, Brown DM, Zhang Z, Segura MP, Weimar T, et al. Absence of branches from xylan in Arabidopsis gux mutants reveals potential for simplification of lignocellulosic biomass. Proc Natl Acad Sci USA. 2010;107:17409–14.
52. Lee C, Teng Q, Zhong R, Ye ZH. Arabidopsis GUX proteins are glucuronyltransferases responsible for the addition of glucuronic acid side chains onto xylan. Plant Cell Physiol. 2012a;53:1204–16.
53. Rennie EA, Hansen SF, Baidoo EE, Hadi MZ, Keasling JD, Scheller HV. Three members of the Arabidopsis glycosyltransferase family 8 are xylan glucuronosyltransferases. Plant Physiol. 2012;159:1408–17.
54. Persson S, Caffall KH, Freshour G, Hilley MT, Bauer S, Poindexter P, et al. The Arabidopsis irregular xylem8 mutant is deficient in glucuronoxylan and homogalacturonan, which are essential for secondary cell wall integrity. Plant Cell. 2007;19:237–55.
55. Lee C, Zhong R, Richardson EA, Himmelsbach DS, McPhail BT, Ye. Z H.The PARVUS gene is expressed in cells undergoing secondary wall thickening and is essential for glucuronoxylan biosynthesis. Plant Cell Physiol. 2007b;48:1659–72.
56. Lee C, Teng Q, Huang W, Zhong R, Ye ZH. The F8H glycosyltransferase is a functional paralog of FRA8 involved in glucuronoxylan biosynthesis in Arabidopsis. Plant Cell Physiol. 2009b;50:812–27.
57. Raes J, Rohd A, Christensen JH, Peer YV, Boerjan W. Genome-wide characterization of the lignification toolbox in Arabidopsis. Plant Physiol. 2003;133:1051–71.
58. Shi R, Sun YH, Li Q, Heber S, Sederoff R, Chiang VL. Towards a systems approach for lignin biosynthesis in Populus trichocarpa: transcript abundance and specificity of the monolignol biosynthetic genes. Plant Cell Physiol. 2010;51:144–63.
59. Vanholme R, Morreel K, Darrah C, Oyarce MP, Grabber JH, Ralph J, Boerjan MW. Metabolic engineering of novel lignin in biomass crops. New Phytol. 2012;196:978–1000.
60. Wang W, Zhang J, Ge H, Li S, Li X, Yin X, Grierson D, Chen K. EjMYB8 transcriptionally regulates flesh lignification in loquat fruit. PLoS One. 2016;11(4):e0154399. doi:10.1371/journal.pone.0154399.
61. Li H, Suo J, Han Y, Liang C, Jin M, Zhang Z, Rao J. The effect of 1-methylcyclopropene, methyl jasmonate and methyl salicylate on lignin accumulation and gene expression in postharvest ‘Xuxiang’ kiwifruit during cold storage. Postharvest Biol Technol. 2017;124:107–18.
62. Bonawitz ND, Chapple C. The genetics of lignin biosynthesis: connecting genotype to phenotype. Annu Rev Genetics. 2010;44:337–63.
63. Lu S, Li Q, Wei H, et al. Ptr-miR397a is a negative regulator of laccase genes affecting lignin content in Populus trichocarpa. PNAS. 2013;110(26):10848–53.

64. Herrero J, Fernández-Pérez F, Yebra T, et al. Bioinformatic and functional characterization of the basic peroxidase 72 from Arabidopsis thaliana involved in lignin biosynthesis. Planta. 2013;237:1599–612.
65. Shigeto J, Kiyonaga Y, Fujita K, Kondo R, Tsutsumi Y. Putative cationic cell-wall-bound peroxidase homologues in Arabidopsis, AtPrx2, AtPrx25, and AtPrx71, are involved in lignification. J Agri Food Chem. 2013;61:3781–8.
66. Gavnholt B, Larsen K. Molecular biology of plant laccases in relation to lignin formation. Physiol Plant. 2002;116:273–80.
67. Berthet S, Demont-Caulet N, Pollet B, et al. Disruption of LACCASE4 and 17 results in tissue-specific alterations to lignification of Arabidopsis thaliana stems. Plant Cell. 2011;23:1124–37.
68. Zhao Q, Tobimatsu Y, Zhou R, Pattathil S, Gallego-Giraldo L, Fu C, Jackson LA, Hahn MG, Kim H, Chen F, et al. Loss of function of cinnamyl alcohol dehydrogenase1 leads to unconventional lignin and a temperature-sensitive growth defect in Medicago truncatula. PNAS. 2013;110:13660–5.
69. Shigeto J, Itoh Y, Hirao S, Ohira K, Fujita K, Tsutsumi Y. Simultaneously disrupting AtPrx2, AtPrx25 and AtPrx71 alters lignin content and structure in Arabidopsis stem. J Integr Plant Biol. 2015;57:349–56.
70. Fry SC. Oxidative coupling of tyrosine and ferulic acid residues: intra- and extra-protoplasmic occurrence, predominance of trimers and larger products, and possible role in inter-polymeric cross-linking. Phytochem Rev. 2004;3:97–111.
71. Novo-Uzal E, Fernandez-Perez F, Herrero J, Gutierrez J, Gomez-Ros LV, Bernal MA, Diaz J, Cuello J, Pomar F, Pedreno MA. From Zinnia to Arabidopsis: approaching the involvement of peroxidases in lignification. J Exp Bot. 2013;64:3499–518.
72. Blokhina OB, Chirkova TV, Fagerstedt KV. Anoxic stress leads to hydrogen peroxide formation in plant cells. J Exp Bot. 2001;52:1179–90.
73. Kotula L, Ranathunge K, Schreiber L, Steudle E. Functional and chemical comparison of apoplastic barriers to radial oxygen loss in roots of rice (Oryza sativa L.) grown in aerated or deoxygenated solution. J Exp Bot. 2009;60:2155–67.
74. Gechev TS, Van Breusegem F, Stone JM, Denev I, Laloi C. Reactive oxygen species as signals that modulate plant stress responses and programmed cell death. Bioessays. 2006;28:1091–101.
75. Raiskila S, Pulkkinen M, Laakso T, Fagerstedt K, Löija M, Mahlberg R, Paajanen L. Ritschkoff A C and Saranpää P. FTIR Spectroscopic prediction of klason and acid soluble lignin variation in Norway spruce cutting clones. Silva Fenn. 2007;41:351–71.
76. Xiong SM, Zuo XF, Zhu YY. Determination of cellulose, hemicellulose and lignin in rice hull. Cerealï¼Feed industry. 2005;8:40–1. (In Chinese).
77. Mao SM, Xu JZ, Zhou SF, Zhang YQ, Liu YH. Determination of polysaccharide from Lonicera japonica at different flowering phases by phenol-sulfuric acid method. Central South Pharmacy. 2015;13(1):65–7. (In Chinese).

# Declarations

**Ethics approval and consent to participate** Not applicable

**Consent for publication** Not applicable

**Availability of data and materials**

 The raw data of transcription sequencing generated during the current study are available in the [NCBI Bioproject] repository, [https://www.ncbi.nlm.nih.gov/bioproject/PRJNA588520]

 The raw data of proteome sequencing generated during the current study are available in the [iProX] repository, [https://www.iprox.org/page/project.html?id=IPX0002167000], It also can be found in the [ProteomeXchange] repository, [http://proteomecentral.proteomexchange.org/cgi/GetDataset?ID=PXD018829].

 All data analyzed during this study are included in this published article [and its supplementary information files].

**Competing interests** The authors declare that they have no competing interests.

**Funding:** This research was funded by the National Natural Science Foundation of China (grant 31760565) and Natural Science Foundation of Xinjiang Province (CN) (grant 2019D01A63). Funders have no role in the design of the study and collection, analysis, and interpretation of data and in writing the manuscript.

**Authors' contributions: AM, XLZ, a**nd **JX** designed the research. **AM, XLZ,** and **PY** performed most of the experiments and analyzed the data. **AM** wrote the manuscript. **PY, CM,** and **JXW** participated to the result analyses and interpretation of data. **JX** revised the manuscript critically. All authors have read and approved the final manuscript.

**Acknowledgements:** We would like to thank members of the Novogene Bioinformatics Technology Co., Ltd for technical sport for proteomic and transcriptomic sequencing. We thank members of our team for fruitful discussions, technical assistance and constructive advices.

# Figures

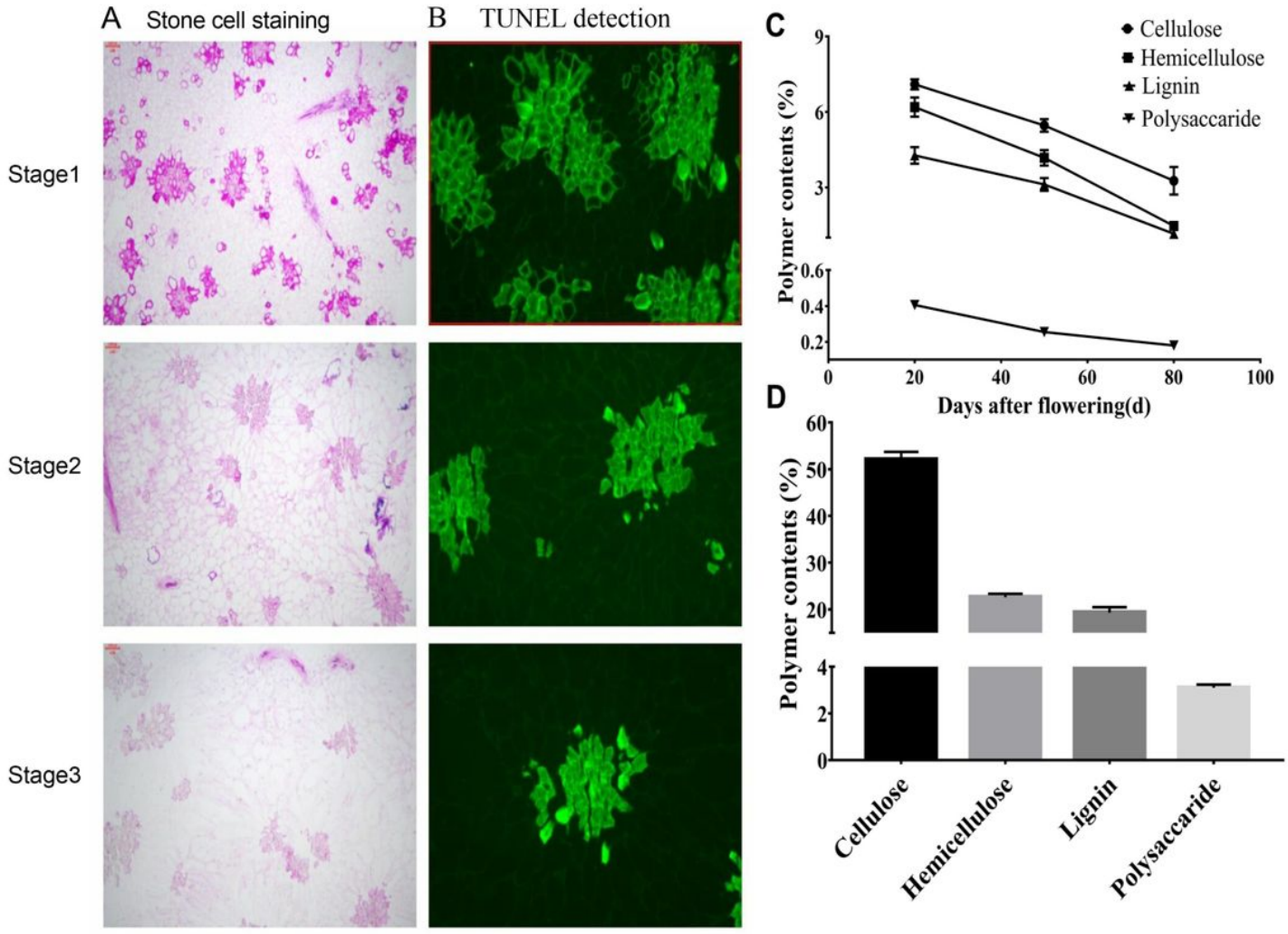


## Figure 1

Morphological and physiological differences in Korla pear pulp during the experimental time courses. (A) 0.1% Safranin staining results of stone cells; (B) TUNEL detection of pear fruit cell apoptosis during experimental time course. (C) Variation in cell wall polymers during development (C), and composition of stone cells (D). Bars represent mean ± SD (n=3).

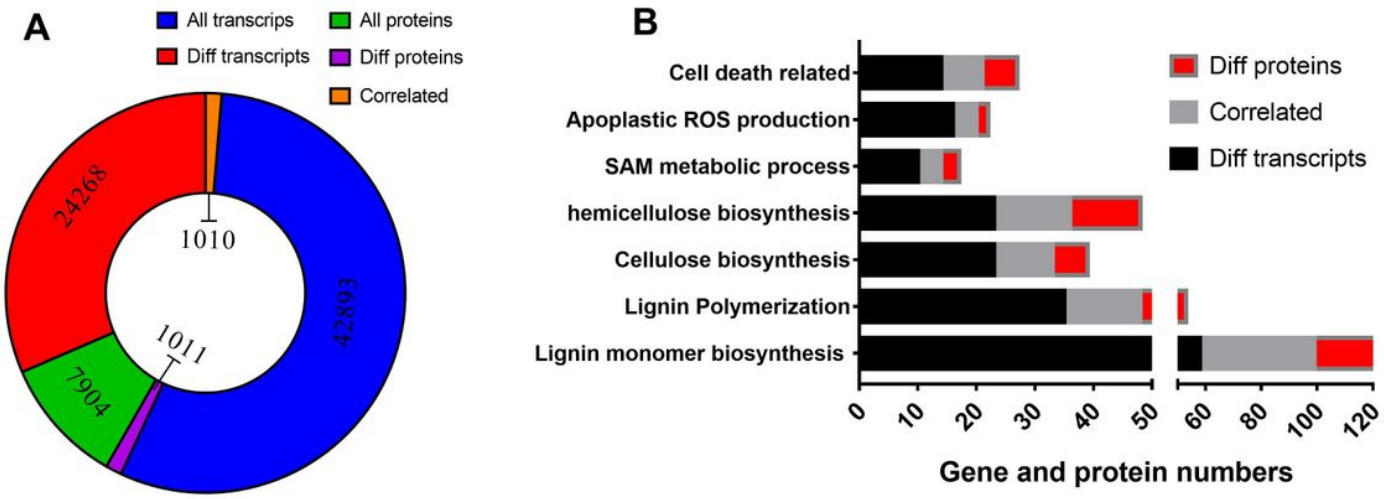


## Figure 2

Overview of transcriptome and proteome data. (A)The circular graph showing the total genes and proteins, DEGs and DAPs as well as correlated genes and proteins identified. (B) The bar chart listing the pathways of interest, and the number of differentially expressed genes and proteins enriched to these pathways.

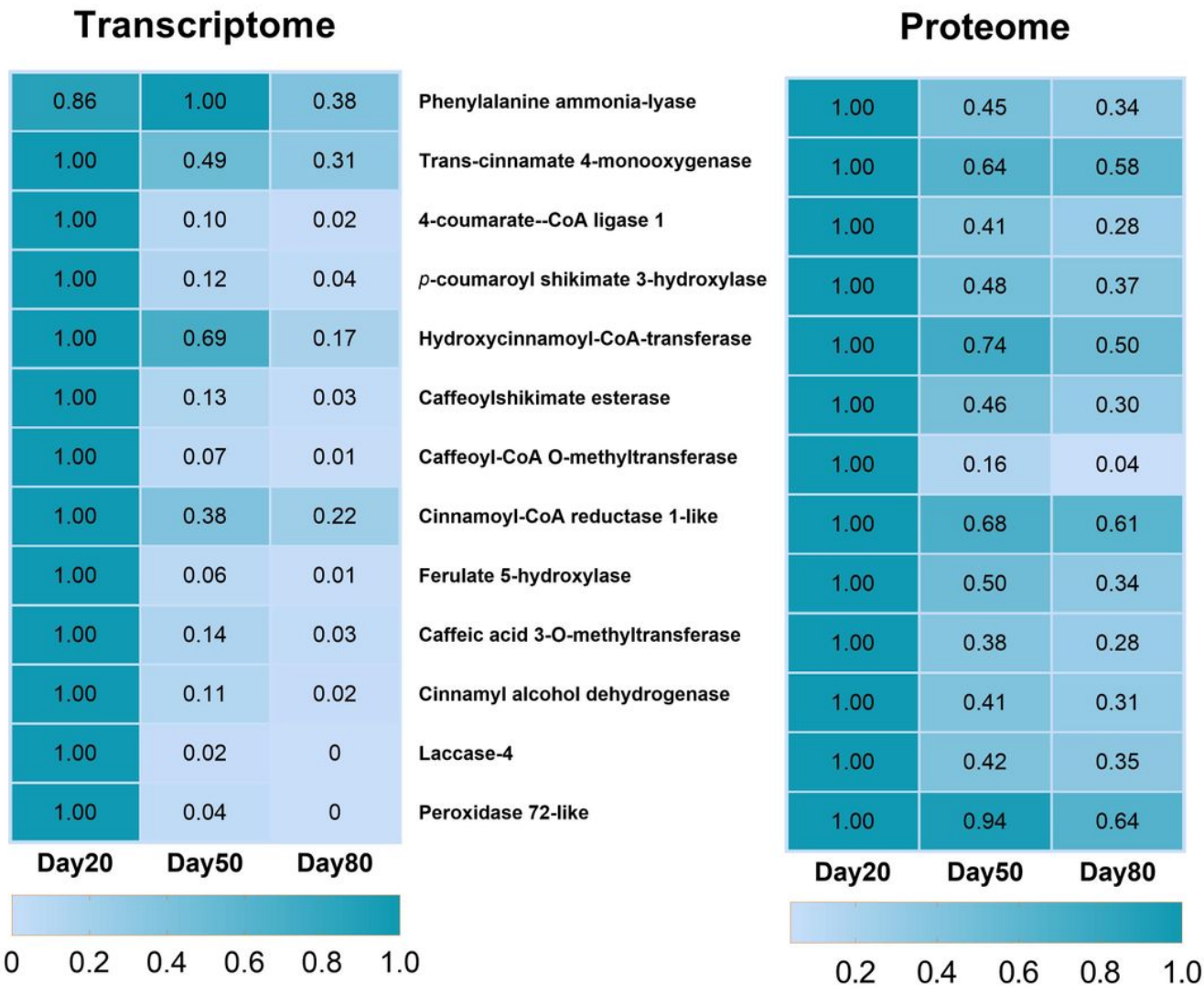


## Figure 3

Expression of genes and proteins involved in lignin biosynthetic process. Heat maps were produced using standardized figures that were transformed to a value between 0.0 and 1.0 by Min-Max normalization method.

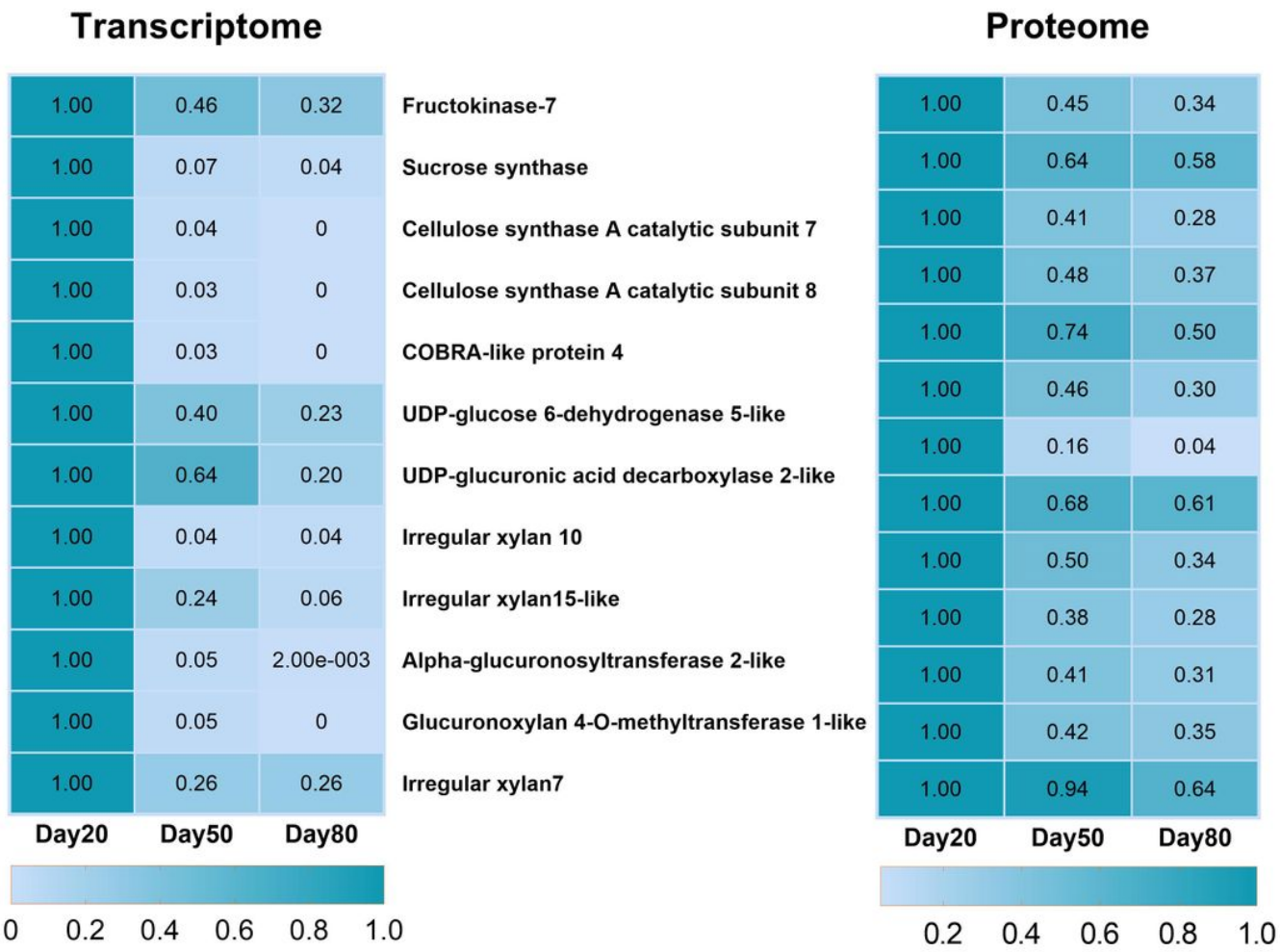


## Figure 4

Genes and proteins involved in cellulose and xylan biosynthesis. Heat maps were produced using standardized figures that were transformed to a value between 0.0 and 1.0 by Min-Max normalization method.

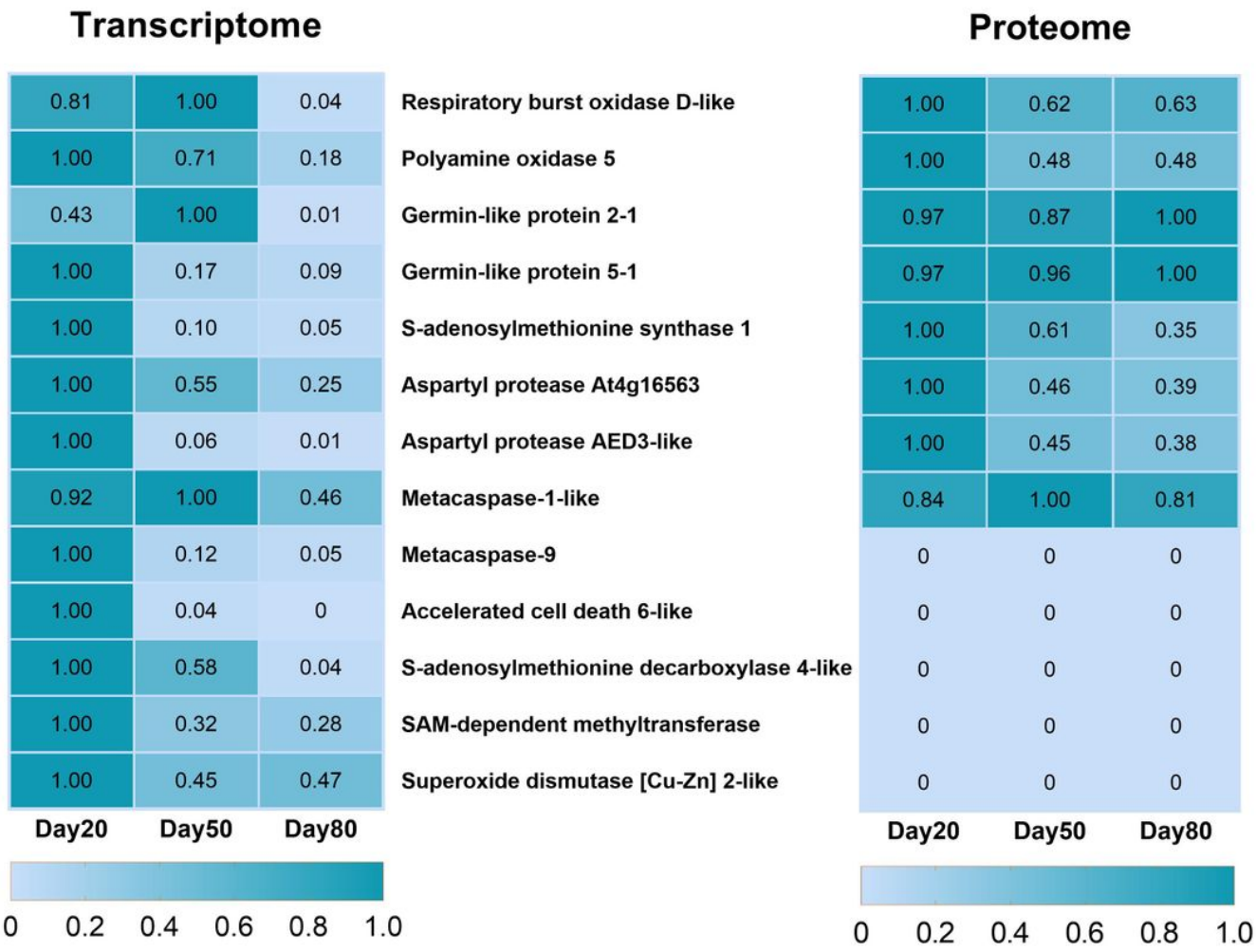


**Figure 5**

Other genes and proteins involved in apoplastic ROS production、SAM metabolic process and programmed cell death. Heat maps were produced using standardized figures that were transformed to a value between 0.0 and 1.0 by Min-Max normalization method. In the proteome data, the 0 value for all three periods representing that no corresponding protein was detected.

# Supplementary Files

This is a list of supplementary files associated with this preprint. Click to download.

- Supplementarymaterials.rar
- Figures.rar